-RESEARCH PAPER-

International Journal of Mining and Geo-Engineering

IJMGE

IJMGE 27-1 (2023) 65-71

DOI: 10.22059/IJMGE.2022.340418.594955

# Performance of T-shaped skirted footings resting on sand

Tammineni Gnananandarao [a], Kennedy Onyelowe [b, *], Vishwas Nandkishor Khatri [c] and Rakesh Kumar Dutta [d]

[a] *Department of Civil Engineering, Aditya College Engineering & Technology, ADB Rd, Surampalem, Andhra Pradesh, India*

[b] *Department of Civil Engineering, Michael Okpara University of Agric., Umudike, Nigeria*

[c] *Department of Civil Engineering, Indian Institute of Technology, Dhanbad, India*

[d] *Department of Civil Engineering, National Institute of Technology, India*

Article History:

Received: 12 March 2022

Revised: 26 August 2022

Accepted: 22 October 2022

## ABSTRACT

A series of plate load tests were performed on a model T-shaped skirted footing by varying the normalized skirt depth and relative density of sand from 0.25 to 1.5 and 30 % to 60 %, respectively. The findings revealed that, regardless of the roughness condition, the observed peak in the pressure settlement ratio corresponding to relative densities of 30%, 40%, 50%, and 60% gradually vanished as the normalized skirt depth was increased from 0.25 to 1.5. The results further revealed that at a given pressure, a lesser settlement ratio was observed for a skirted footing than the footing without a skirt. The most significant benefit of providing a skirt to the footing was obtained when the base and skirt were partially rough and the relative density of sand was kept at 30%. In all the cases, the observed bearing capacity ratio for the present skirted footing was higher than the H-shaped skirted footing reported in the literature. Finally, an empirical equation was proposed to predict the bearing capacity ratio and settlement reduction factor for a given skirt depth and sand relative density.

**Keywords:** *Bearing capacity ratio, Settlement reduction factor, Multi-edge skirted footing, Sand, relative density, Roughness, Multivariable regression*

## 1. Introduction

In Geotechnical engineering practice, the conventional shapes (square, circular, and rectangular) of shallow and deep foundations were employed. These foundations distribute loads to the underlying soil by end bearing (in the case of a shallow foundation) or end bearing and skin friction (in the case of a deep foundation) together. Furthermore, the floating foundation is designed to balance the weight of the structure built with that of excavated soil. But there can be certain circumstances where the footing with different geometries such as Cross, T- and H-shape in the plan is required due to economic and architectural reasons. Such footings were termed multi-edge footings, as reported by [1-2]. According to a laboratory test on multi-edge footings conducted by [2], the bearing capacity of the multi-edge footings was somewhat greater than the bearing capacity of the square footing of the same width. A numerical study using finite difference code FLAC 3D was performed by [3] to study the failure behavior of the soil beneath the multi-edge footing without a skirt. Over the years, researchers [4-10] focused on using skirts attached to conventional shallow footings to improve the bearing capacity and reduction in the settlement. The other technique to reduce settlement below the superstructure is reported by [11]. Skirted footings were traditionally used for offshore structures [12-15]. On the other hand, its use in typical shallow footings has increased nowadays as it results in a significant increase in bearing capacity and a reduction in the settlement at a given pressure compared to a footing without skirts under identical ground and loading conditions. Due to the benefits of using skirted footings, particularly in loose sand, it can also be considered an alternative ground improvement technique, as reported by [9, 16].

Furthermore, footings can be installed on the ground without excavation for the foundation pit, even in the presence of a water table [9]. A study on the H-shaped skirted footing was recently reported by [17] by varying the relative density and the normalized skirt depth from 30 % to 60 % and 0.25 to 1.5, respectively. They confirmed the findings of [2] about multi-edge footings without skirts. However, there is a lack of research regarding T-shaped skirted footing in literature. The present paper evaluates the performance of the T-shaped footing with and without a skirt by conducting a laboratory plate load test. The results obtained in this study were analyzed using multiple regression analysis. The equations were proposed to predict the bearing capacity ratio and settlement reduction factor for T-shaped footing with the skirt.

## 2. Materials Used and Experimental Procedure

The sand used in this study was collected from a place near Hamirpur (31.63°N, 76.52°E), Himachal Pradesh, India. The sand had a specific gravity of 2.67 and was classified as poorly graded (SP) following [18]. The maximum and minimum dry unit weights of sand were 15.97 kN/m$^3$ and 13.06 kN/m$^3$, respectively. The properties of the sand were depicted in Table 1. The sand was washed to remove the fines and the organic matter before performing the experimental study. The relative density chosen in this study varied from 30 % to 60 %, following the literature [19, 20]. The consolidated drained triaxial test was performed at a relative density of 30 %, 40 %, 50 %, and 60 %. The p'-q' plot is shown in Figure 1. The curves were plotted to correspond to peak values. The friction angle corresponding to a relative density of 30 %, 40 %, 50 %,

* Corresponding author. *E-mail address:* kennedychibuzor@kiu.ac.ug (K. Onyelowe).

and 60 % was determined as 36.06°, 38.64°, 39.86°, and 41.72°, respectively.

The T-shaped footing and the skirt were prepared using 10 mm and 5 mm thick steel plates, respectively. The footing and skirt's rigid behavior were anticipated with the selected thickness. The skirt was precisely and firmly welded under the base of the T-shaped footing around the perimeter using a steel plate carved into a T shape. The selected skirted footing configuration represents field conditions in which (i) the skirts were installed in the ground rigidly connected to the footing or (ii) the skirts were installed first, followed by the installation of the footing on top of the skirts and firmly connected to the same. The normalized skirt depths adopted for the study of regular-shaped footings in literature [8-9, 19-21] were in the range of 0.05 to 2. Keeping this in mind, the normalized skirt depth ($D_s$/B) in this study varied from 0.25 to 1.5, where $D_s$ is the skirt depth and $B$ is the width of the footing. The flange width (B) and overall depth (L) for the footing was kept at 80 mm. The flange thickness and the web of the footing were 26 mm each, and the area of the footing was 3500 mm$^2$. Figure 2 depicts the schematic of the T-shaped footing with and without a skirt. The footing and the skirt were made rough by gluing the sand particles to the base of the footing and the inner surfaces of the skirt. Whereas for the partly rough condition, no such sand particles were glued to the bottom of the footing or the inner surfaces of the skirt. The details of the skirted footings used in actual practice reported by [22] are provided in Table 2.

The interface friction angle ( ) was determined from the modified direct shear test for both partial rough and rough conditions corresponding to a relative density of 30 %, 40 %, 50 %, and 60 %. The plots for shear stress versus deformation are shown in Figure 3 and Figure 4, respectively, for the partly rough and rough conditions of the footing at different relative densities. The interface friction angles ( ) were 22.90°, 23.61°, 24.51°, and 27.32° for partly rough footing conditions, as well as 36.46°, 38.07°, 39.03°, and 40.66° for rough footing conditions corresponding to a relative density of 30 %, 40 %, 50 %, and 60 %, respectively. However, in the present study, both the friction angle ( ) and interface friction angle ( ) were obtained corresponding to the peak values of the stress. Further, the applied minor principal stress ranged between 24.252 kPa to 196.2 kPa for determining the friction angle of the sand, whereas for the interface friction angle, the applied normal stress was in the range of 49.05 kPa to 196.2 kPa. It is pertinent to mention here that the ratio for; the partly-rough condition was 0.60-0.65, whereas, for the completely rough condition, it was close to 1.

The model tests were performed in a test tank having dimensions 700 mm (length) × 450 mm (width) × 600 mm (depth). The dimensions of the test tank were selected to ensure the pressure-settlement behavior of the footing was not affected by the presence of rigid boundary conditions. The tank was filled with eight equal layers of 60 mm each to a height of 480 mm to prepare the sand bed. The weight of the sand to a given relative density was calculated for each layer, poured from a constant height to fill the given layer, and compacted manually using a wooden rammer of 6 N. The number of required blows for compaction for a given relative density was arrived at by trial and error. It was ensured that the difference in measured relative densities was within ± 1 %. The test on the prepared sand bed was performed with a strain-controlled loading frame of 50000 N and a load cell of 5000 N capacity. The photograph of the test setup and the T-shaped footing is shown in Figure 5. All the tests were carried out at a strain rate of 0.24 mm/min. For testing footing without a skirt, the model footing was placed on the surface of the prepared bed. The plunger for the load application was brought in contact with the metal ball placed on the top of the footing at the center of gravity (Figure 5 (b)) before continuing the load test. In the case of footing with a skirt, following [9], the footing was pushed into the sand (Figure 5 (c)) by applying the load till the footing base was just in contact with the top surface of the sand. No heave was noticed around footing by such placement procedure as reported by [9] for the conventional footing. It implies that the marginal densification of the sand around the skirt periphery may not significantly affect the ultimate bearing capacity of the footing.

**Table 1.** Properties of sand.

| Description | Values |
|---|---|
| $D_{10}$ (mm). | 0.15 |
| $D_{30}$ (mm) | 0.18 |
| $D_{50}$ (mm) | 0.2 |
| $D_{60}$ (mm) | 0.22 |
| Coefficient of uniformity, $C_u$ | 1.46 |
| Coefficient of curvature, $C_c$ | 0.98 |
| Classification | SP |
| Maximum dry unit weight (kN/m$^3$) | 15.97 |
| Minimum dry unit weight (kN/m$^3$) | 13.06 |
| Specific gravity | 2.67 |

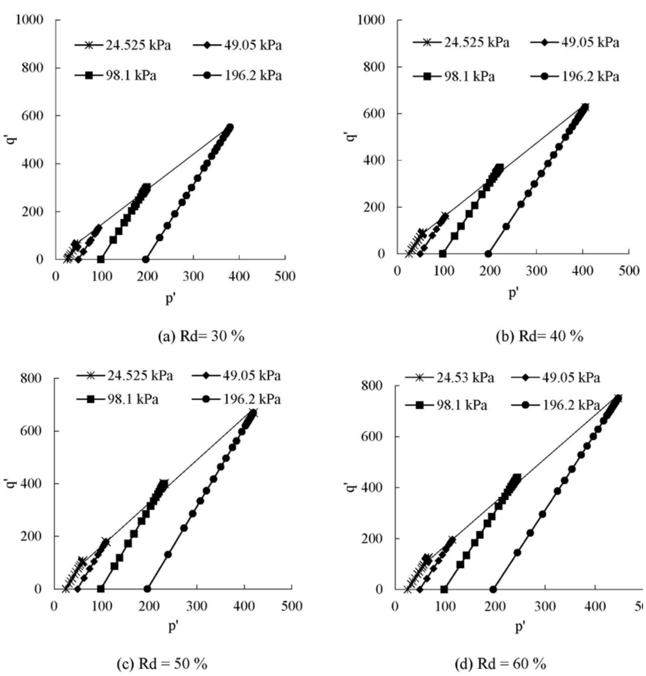


**Figure. 1.** p'-q' plot of the sand at various relative density

**Table 2.** Details of skirted footings used in practice (after [22]).

| Project name and year | Type of foundation | Location | Soil condition | Foundation in plan | Foundation dimensions | Skirt depth | Normalised skirt depth |
|---|---|---|---|---|---|---|---|
| Heidrun 1995 | Tension leg platforms | North Sea, Norway | Soft clay with boulders | 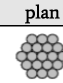 | A = 1504 m$^2$ D = 9 m | 4.6 m | 0.51 |
| Wandoo 1997 | Gravity based structures | Northwest shelf, Australia | Thin layer dense calcareous sand | 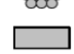 | A = 7866 m$^2$ D = 100 m | 0.3 m | 0.003 |
| Bayu Undam 2003 | Jacket with steel plates | Timor sea, Australia | 2 m very soft calcareous sandy silt over cemented calcarenite and limestone |  | $A_{total}$ = 480 m$^2$ $A_{plate}$ = 120 m$^2$ 6 m x 20 m | 0.5 m | 0.04 |
| Yolla 2004 | Skirted gravity-based structures /jacket hybrid | Bass Strait, Australia | Firm calcareous sandy silt with very soft clay and sand layers |  | A = 2500 m$^2$ 50 m x 50 m D = 56.4 m | 5.4 m | 0.1 |

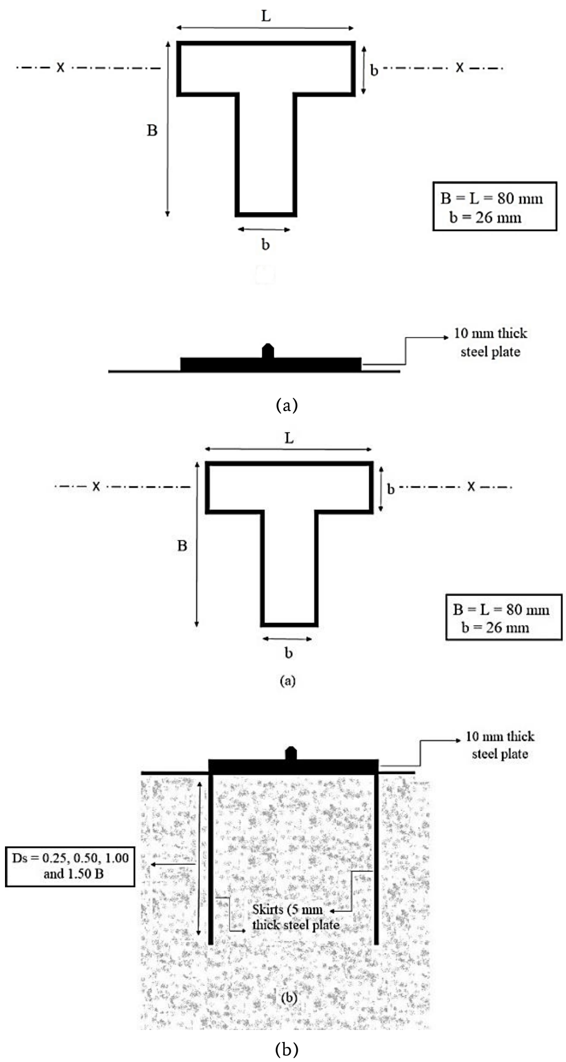


**Figure 2.** T shaped footing (a) without skirt (b) with skirt.

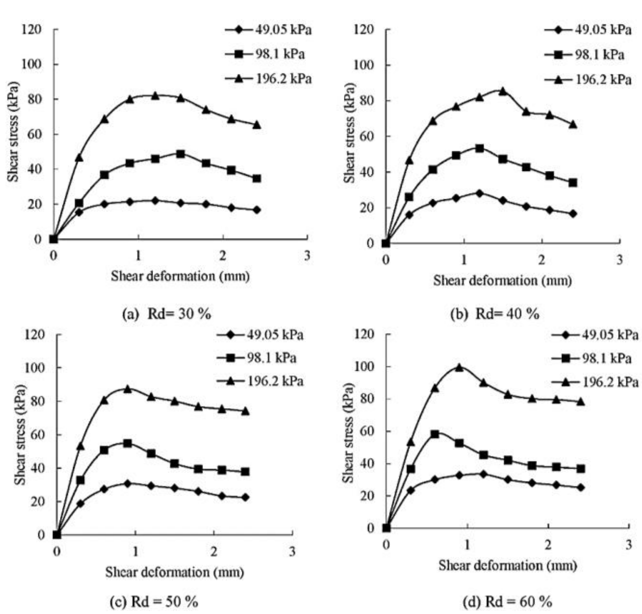


**Figure 3.** Shear stress versus shear deformation plots at different relative density with a partly rough interface.

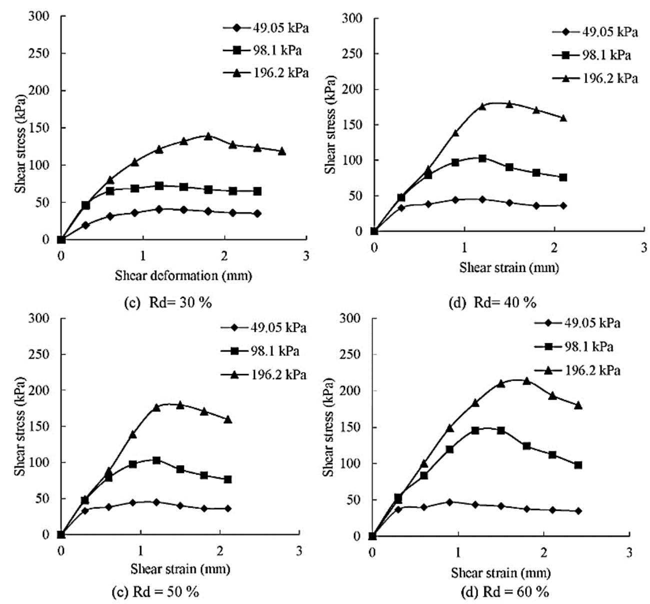


**Figure 4.** Shear stress versus shear deformation plots at different relative density with a rough interface

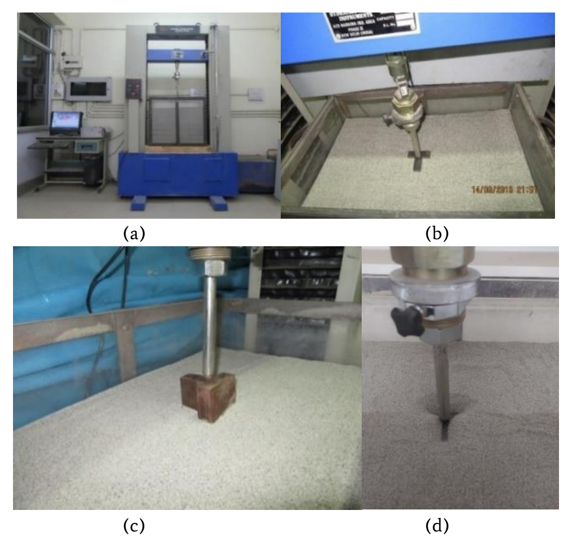


**Figure 5.** Photograph of the (a) test setup (b) T-shaped footing without skirt (c) pushing T-shaped footing into sand (d) T-shaped footing at failure.

The test was then continued like the footing without a skirt. The failure point of skirted footing after the test is presented in Figure 5 (d). All the tests were carried out up to an *S/B* ratio of 30 %, where *S* and *B* were settlement and the width footing. The load-settlement observations were recorded digitally with a data logger for each test. Each test was performed thrice to ensure the repeatability of the test results.

## 3. Results

### *3.1. Pressure-Settlement Ratio Behaviour of Multi-Edge T-Shaped Footings with and without Skirt*

Forty tests were conducted by varying the normalized skirt depth, relative density, and the roughness of the base of the footing and the inner surfaces of the skirt to analyze the performance of the footings. Figure 6 displays the pressure-settlement ratio curves for the footing with and without a skirt. The addition of a skirt to the T-shaped footing significantly improved the pressure-settlement ratio behavior of this figure, according to research on it. For example, a clear peak was observed corresponding to a relative density of 30 %, 40 %, 50 %, and 60 %, both for the rough and partly rough conditions for the footing without a skirt, indicating a general shear failure. Sand being confined between the angles of the T-shape, the general shear failure is produced at all relative densities. Further, due to the dilatancy effect, a peak can be observed in all the experimental conditions at all relative densities and roughness within the short settlement ratio (*S/B*), as evident from Figure 6.

The average settlement ratio (*S/B*) at failure for the multi-edge T-shaped footing without a skirt was about 7 % for the partly rough and rough conditions. It implies that the observed behavior was independent of the roughness condition of the footing without a skirt. This observation was consistent with the literature [17] regarding the multi-edge H-shaped footing. With the addition of the skirt to the footing, the clear peak observed in the pressure settlement ratio curve corresponding to a relative density of 30 %, 40 %, 50 %, and 60 %, as evident from Figure 6, gradually vanished with the increase in the normalized skirt depth (*Ds/B*) from 0.25 to 1.5 indicating a local shear failure. This is attributed to the localized failure pattern below the tip of the skirt. The observed behavior regarding skirted footing was independent of the roughness condition of the base as well as the inner surfaces of the skirt. This observation was consistent with the literature [17] regarding the multi-edge H-shaped footing. A close examination of Figure 6 further reveals that at a given pressure, a lesser settlement ratio (*S/B*) was observed for the skirted footing compared to the footing without a skirt. This observation was consistent with all the relative densities, the normalized skirt depth, and the roughness condition.

### 3.2. Effect of Skirt Depth on the Bearing Capacity

As shown in Figure 6, the bearing capacity of the footing was determined from the pressure-settlement ratio curve. The bearing capacity was taken corresponding to a peak pressure or a pressure corresponding to *S/B* of 10 %, whichever occurs earlier. Additionally, if the clear peak was not visible in the pressure-settlement ratio curve, the bearing pressure was obtained using the double tangent method and adopted as peak pressure. The same was compared with the pressure corresponding to *S/B* = 10%. The bearing capacity variation for footing without a skirt is tabulated in Table 3. For the skirted footing, the bearing capacity was expressed as a ratio by dividing its magnitude by the bearing capacity of the un-skirted footing. The bearing capacity ratio (BCR) at different relative densities and normalized skirt depth is shown in Table 3. The study of this table reveals that adding a skirt to the multi-edge T-shaped footing significantly improved the bearing capacity ratio for the partly rough and rough conditions. For instance, the bearing capacity ratio of the partly rough and rough condition of the footing resting on the sand with a relative density of 30 % and normalized skirt depth of 0.25 was 1.67 and 1.44, respectively. With an increase in the normalized skirt depth to 1.5, the bearing capacity ratio of the footing increased to 3.86 and 3.28, respectively, at the same relative density.

Further, from Table 3, the bearing capacity ratio of the partly rough and rough condition of the footing resting on the sand having a relative density of 60 % and normalized skirt depth of 0.25 was 1.34 and 1.26, respectively. With the normalized skirt, depth increased to 1.5, and the bearing capacity ratio of the footing increased to 2.68 and 2.41, respectively, at the same relative density. It is pertinent to mention that the bearing capacity for the multi-edge T-shaped footing without a skirt was higher for the rough condition than the partly rough condition. The higher bearing capacity for the multi-edge T-shaped footing under rough conditions was attributed to greater interface friction between the footing and sand compared to the partly rough condition and thus requiring more load to bring the sand to failure. Further, the BCR of the footing under rough conditions was marginally smaller than the BCR of the partly rough-skirted footing for a given relative density of the sand and the skirt depth, as evident from Table 3. This table also reveals that the highest benefit of providing a skirt to the multi-edge T-shaped footing was derived in the case of partly rough-skirted footing at a relative density of 30 %. This observation is consistent with the literature [5-8] regarding the conventional regular-shaped skirted footings. Further study of Table 2 reveals that the bearing capacity ratio decreased with the increase in the relative density of the sand corresponding to a given normalized skirt depth. This observation was consistent with both the roughness condition.

### 3.3. Comparison with Literature

The comparison was attempted for the present multi-edge T-shaped skirted footing with the one available in the literature for the multi-edge H-shaped skirted footing. The bearing capacity for the multi-edge H-shaped skirted footing for the partly rough and rough conditions reported by [17] is shown in Table 4. The values reported in Table 4 were used to calculate the bearing capacity ratio. Figure 7 compares the multi-edged T and H-shaped skirted footing's bearing capacity ratio in rough and partially rough cases. This figure shows that T-shaped skirted footing had a higher bearing capacity ratio than H-shaped skirted footing at all relative densities and normalized skirt depth despite having a lesser footing area (3500 mm$^2$) than that of the former (4900 mm$^2$). The trend was the same irrespective of the roughness of the footing. The bearing capacity of the H-shaped footing without a skirt was higher than the T-shaped footing without a skirt. Hence, a higher bearing capacity ratio in the T-shaped skirt footing is justified.

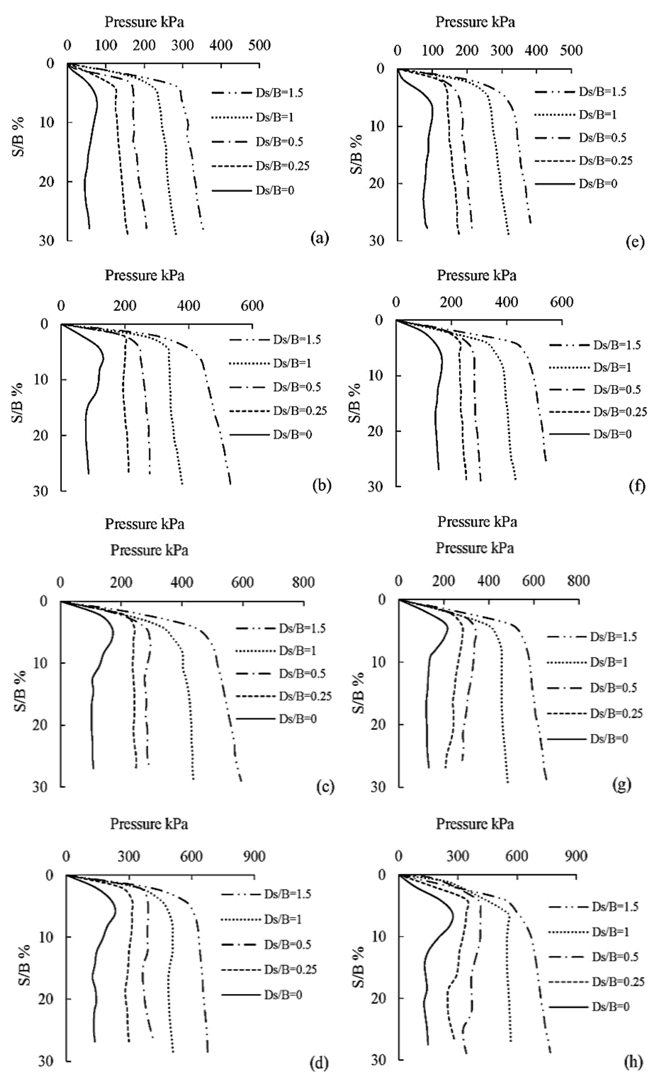


**Figure 6**. Pressure-settlement ratio plot of T-shaped footing with partly rough (a-d) and completely rough (e-h) interface and corresponding to a relative density of 30% (a, e), 40% (b, f), 50% (c, g) and 60% (d, h).

**Table 3.** Bearing capacity and bearing capacity ratio for the multi-edge T-shaped footing at different normalised skirt depth and relative density.

| Relative density (%) | Normalized skirt depth ($D_s/B$) | Bearing capacity (kPa) | | Bearing Capacity Ratio (BCR) | |
|---|---|---|---|---|---|
| | | Partly rough | Rough | Partly rough | Rough |
| 30 | 0 | 77.14 | 100.00 | 1.00 | 1.00 |
| | 0.25 | 128.57 | 144.00 | 1.67 | 1.44 |
| | 0.5 | 171.43 | 182.00 | 2.22 | 1.82 |
| | 1 | 236.00 | 260.00 | 3.06 | 2.60 |
| | 1.5 | 298.00 | 328.00 | 3.86 | 3.28 |
| 40 | 0 | 131.43 | 165.71 | 1.00 | 1.00 |
| | 0.25 | 200.00 | 231.43 | 1.52 | 1.40 |
| | 0.5 | 244.50 | 282.00 | 1.86 | 1.70 |
| | 1 | 340.00 | 384.00 | 2.59 | 2.32 |
| | 1.5 | 430.00 | 482.00 | 3.27 | 2.91 |
| 50 | 0 | 168.57 | 211.43 | 1.00 | 1.00 |
| | 0.25 | 240.00 | 282.86 | 1.42 | 1.34 |
| | 0.5 | 294.29 | 342.86 | 1.75 | 1.62 |
| | 1 | 401.93 | 457.14 | 2.38 | 2.16 |
| | 1.5 | 498.00 | 560.00 | 2.95 | 2.65 |
| 60 | 0 | 234.29 | 271.43 | 1.00 | 1.00 |
| | 0.25 | 314.29 | 342.86 | 1.34 | 1.26 |
| | 0.5 | 391.43 | 414.29 | 1.67 | 1.53 |
| | 1 | 508.57 | 554.29 | 2.17 | 2.04 |
| | 1.5 | 628.00 | 653.00 | 2.68 | 2.41 |

**Table 4.** Bearing capacity of multi-edge H-shaped footing with and without skirt (after [17]).

| Normalised skirt depth ($D_s/B$) | Bearing capacity (kPa) | | | | | | | |
|---|---|---|---|---|---|---|---|---|
| | $R_d$ = 30 % | | $R_d$ = 40 % | | $R_d$ = 50 % | | $R_d$ = 60 % | |
| | Partly rough | Rough | Partly rough | Rough | Partly rough | Rough | Partly rough | Rough |
| 0 | 87.76 | 106.12 | 138.78 | 171.43 | 171.43 | 214.29 | 236.73 | 273.47 |
| 0.25 | 136.73 | 159.18 | 210.20 | 242.86 | 248.98 | 285.71 | 320.41 | 348.98 |
| 0.5 | 171.00 | 197.96 | 259.18 | 298.71 | 302.04 | 344.90 | 393.88 | 418.37 |
| 1 | 248.00 | 270.00 | 352.00 | 400.54 | 414.00 | 462.00 | 513.04 | 561.00 |
| 1.5 | 312.00 | 335.00 | 440.00 | 490.00 | 510.00 | 566.00 | 640.00 | 660.00 |

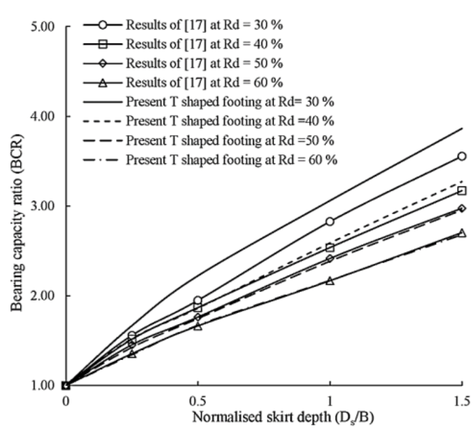


(a)

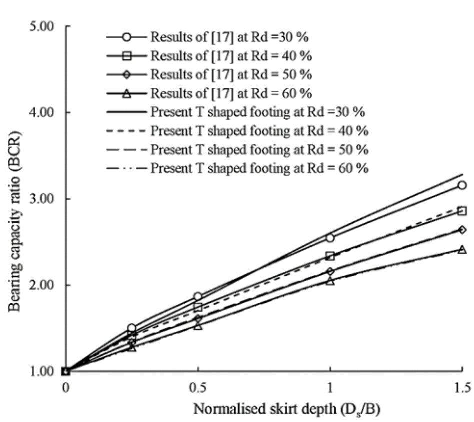


(b)

**Figure 7.** A comparative plot of bearing capacity ratio with the normalised skirt depth at different relative density for (a) partly rough (b) rough condition.

Therefore, the improvement in the bearing capacity ratio of the T-shaped footing with the addition of a skirt was slightly greater than that of the H-shaped skirted footing. However, a detailed numerical study regarding the failure patterns of both footing is required for more insight into this aspect.

## 4. Multiple Regression Analysis for the Prediction of Bearing Capacity Ratio

The multivariable regression analysis of the data reported by [17] in the literature for the square-shaped skirted footing, as shown in Table 5, was used to calculate the bearing capacity ratio. The calculated bearing capacity ratio was used to develop the equation. Choosing the expression's format and utilizing multivariable regression analysis to estimate the BCR, the bearing capacity ratio (BCR) of the regular shaped embedded footing to surface footing can be written as given below:

$$BCR_{Square} = \frac{\gamma D_s N_q s_q d_q + 0.5 B \gamma N_\gamma s_\gamma d_\gamma}{0.5 B_\gamma N_\gamma s_\gamma} \tag{1}$$

Following [23], the $N = 2(N_q + 1)$ tan however, if we assume $N = 2N_q$, the above expression becomes

$$BCR_{Square} = \frac{D_s}{B}\frac{s_q d_q}{S_\gamma \tan\phi} + d_\gamma \tag{2}$$

It implies that the regression expression should be of the following form

$$BCR_{Square} = \frac{D_s}{B}\frac{A}{f(\phi)} + C \tag{3}$$

Where f ( ) is a function of friction angle, and A and C are constants that will be determined from the regression analysis. The skirted footing's BCR expression was chosen based on the expressions of the embedded and skirted footings. However, it was anticipated that the skirted footing's BCR would be slightly higher than the corresponding embedded footing due to the mobilization of the shear resistance along the skirt-soil interface. Using the calculated bearing capacity ratio from the bearing capacity values reported by [17] in Table 5 for the square footing with a skirt, the empirical expression obtained from the regression analysis is given below.

$$BCR_{square} = 44.15\left(\frac{D_s}{B}\right)\left(\frac{1}{r\phi}\right) + 1.07 \tag{4}$$

The constants $A$ and $C$ mentioned in equation (3) were determined as 44.15 and 1.07, respectively, by performing the multiple regression analysis. Further, the magnitude of r for the partly rough and rough conditions was observed at 0.83 and 1 when all the parameters (BCR square, Ds/B, and) and the values of the constants A and C were kept constant. Additionally, using multiple regression analysis, the bearing capacity ratio discovered for the multi-edge T-shaped skirted footing in this study was correlated to the bearing capacity ratio discovered from the square skirted footing reported by [17]. The coefficient found from this analysis was 1.03 for the multi-edge T-shaped skirted footing, and the obtained expression was as follows.

$$BCR_{T\ Footing} = 1.03 \times BCR_{square} \tag{5}$$

A comparison of the predicted and the experimental bearing capacity ratio is shown in Figure 8, indicating that the coefficient of determination ($R^2$) for the various cases lies in the range of 0.92 to 0.95, which is acceptable. Further, the developed regression analysis expression predicts the BCR of the multi-edge T-shaped skirted footing with a maximum deviation of 13.49 % concerning experimental observation.

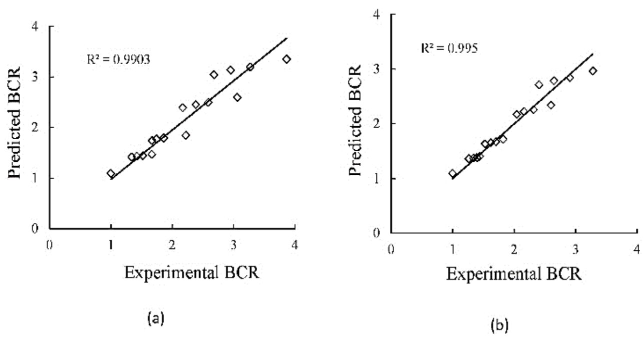


**Figure 8**. Comparison between targeted and predicted bearing capacity ratio for the T shaped skirted footing under (a) partly rough (b) rough condition.

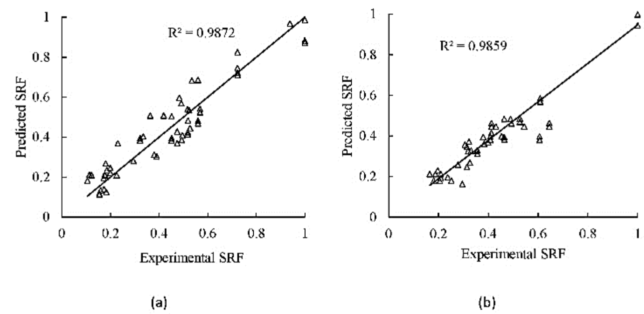


**Fig.ure 9.** Comparison between targeted and predicted settlement reduction factor for the T shaped skirted footing under (a) partly rough (b) rough condition.

## 5. Settlement Reduction Factor

The settlement reduction factor (SRF) is defined as a ratio of the difference between the un-skirted square footing settlement (S) and the skirted square footing settlement (Ssk) to the un-skirted square footing settlement (S). This parameter was developed using the multivariable regression analysis on the data reported by [17] in literature for the square-shaped skirted footing. This equation was evaluated for bearing pressures of 25, 50, 100, 150, and 200 kPa. Three hundred data points were generated, which were not included here due to their vast amount. Following [6], an equation to predict the SRF of the square skirted footing using multivariable regression analysis is obtained and given below.

$$SRF_{square} = e^{\left(1.32r\phi - 0.09\frac{D_s}{B} + 0.03\sigma + 69.44\right)} \tag{7}$$

Further, using multiple regression analysis, the SRF obtained for the T-shaped skirted footing in this investigation was correlated to the SRF of the square skirted footing. The coefficient obtained from this analysis was 0.98 for the multi-edge T-shaped skirted footing, and the obtained expression is given below.

$$SRF_{T\ Footing} = 0.98 \times SRF_{square} \tag{8}$$

A comparison of predicted SRF with the experimental value, as shown in Figure 9, indicates a coefficient of determination ($R^2$) for various cases lies in the range of 0.940 to 0.942, which implies a good fit. Further, a lesser settlement ratio was observed for the T-shaped skirted footing compared to the footing without a skirt at a given pressure.

**Table 5**. Bearing capacity of square footing with and without skirt (after [17]).

| Normalised skirt depth ($D_s/B$) | Bearing capacity (kPa) | | | | | | | |
|---|---|---|---|---|---|---|---|---|
| | $R_d$ = 30 % | | $R_d$ = 40 % | | $R_d$ = 50 % | | $R_d$ = 60 % | |
| | Partly rough | Rough | Partly rough | Rough | Partly rough | Rough | Partly rough | Rough |
| 0 | 65.50 | 73.30 | 120.39 | 153.24 | 158.53 | 207.81 | 228.31 | 268.93 |
| 0.25 | 106.20 | 114.00 | 179.69 | 224.60 | 226.56 | 281.25 | 312.50 | 339.06 |
| 0.5 | 135.00 | 140.00 | 230.00 | 275.00 | 285.94 | 340.63 | 382.81 | 409.38 |
| 1 | 186.00 | 194.00 | 305.00 | 364.05 | 375.00 | 455.37 | 497.72 | 546.08 |
| 1.5 | 230.00 | 239.00 | 375.00 | 440.00 | 456.00 | 535.60 | 593.95 | 640.20 |

## 6. Conclusion

A study on the behavior of multi-edge T-shaped footing with and without a skirt resting on poorly graded sand and subjected to compressive load through a laboratory model study was investigated. Forty model tests were conducted to analyze the enhancement in the bearing capacity and reduction in settlement of a T-shaped footing with and without a skirt. Based on the results following conclusions were drawn:

(1) With the addition of the skirt to the T-shaped footing, the peak pressure observed in the pressure settlement ratio curve gradually vanished with the increase in the normalized skirt depth. Further, the settlement at a given pressure was found to decrease with the increase in the normalized skirt depth. This observation was consistent at different relative densities irrespective of the roughness condition of the footing and the skirt.

(2) The addition of the skirts leads to a substantial increase in the bearing capacity of the footing. The bearing capacity of the skirted footing was observed to be about 1.26 to 3.86 times the bearing capacity of the unskirted footing considering the relative density range, skirt depth, and interface condition.

(3) The maximum benefit of providing a skirt to T-shaped footing was derived when the footing and skirt with the partly rough condition were placed on the sand with a relative density of 30 %.

(4) In all the cases, the bearing capacity of the T-shaped skirted footing was marginally smaller in comparison to the H-shaped skirted

footing. However, the BCR of the T-shaped skirted footing was slightly higher than the H-shaped skirted footing.

(5) Coefficients of determination ($R^2$) for the bearing capacity ratio and settlement reduction factor were in the range of 0.920 to 0.950 and 0.940 to 0.942, respectively, indicating a good fit. The developed regression analysis expression predicts the BCR of the T-shaped skirted footing with a maximum deviation of 13.49 % with respect to experimental observation. A lesser settlement ratio was observed for T-shaped skirted footing than footing without a skirt at a given pressure.

It is anticipated that the present study's outcome will help predict the bearing capacity and the settlement of the multi-edge T-shaped skirted footing.

**Notations**

| | |
|---|---|
| $L$ | Length of footing; |
| $B$ | Width of footing; |
| $b$ | Thickness of flange/ web of plus-shaped footing; |
| $D_s$ | Depth of the structural skirt; |
| $S/B$ | Settlement to footing width ratio; |
| $R_d$ | Relative density of sand; |
| $\Phi$ | Angle of internal friction of sand; |
| $C_u$ | Coefficient of uniformity; and |
| $C_c$ | Coefficient of curvature; |
| $N_\gamma$ and $N_q$ | Bearing capacity factors; |
| $S_\gamma$ and $S_q$ | Shape factors; |
| $d_q$ and $d_\gamma$ | Depth factors; |
| $R^2$ | Coefficient of Determination; |
| r | Roughness coefficient for BCR or SRF; |
| σ | Normal stress |

## REFERENCES


[1] U. Jaiswal and P. Sengupta, Seismic performance of reinforced concrete buildings with plan asymmetry. International Journal of Emerging Technology and Advanced Engineering. 7(2), 246-251. (2017)

[2] B. Dawarci, M. Ornek, Y. Turedi, Analysis of multi-edge footings rested on loose and dense sand. Periodica Politechnica Civil Engineering. 58(4), 355-370 (2014)

[3] M. Ghazavi, S. Mokhtari, Numerical investigation of load-settlement characteristics of multi-edge shallow foundations. The 12th International Conference of International Association for Computer Methods and Advances in Geomechanics. 3344-3351, Goa, India (2008)

[4] M. Y. Al-Aghbari, Y. E. A. Mohamedzein, Bearing capacity of strip foundations with structural skirts. Geotechnical & Geological Engineering. **22**(4), 43-57 (2004)

[5] M.Y. Al-Aghbari, Settlement of shallow circular foundations with structural skirts resting on sand. The Journal of Engineering Research.**4**(1), 11-16 (2007)

[6] M.Y. Al-Aghbari, R.K. Dutta, Performance of square footing with structural skirt resting on sand. Geomechanics and Geoengineering. **3**(4), 271-277 (2008)

[7] A.Z. El Wakil, 2010. Horizontal capacity of skirted circular shallow footings on sand. Alexandria Engineering Journal. **49**, 379-385 (2010)

[8] H.T. Eid, Bearing capacity and settlement of skirted shallow foundations on sand. International Journal of Geomechanics.**13**(5), 645-652 (2013)

[9] V.N. Khatri, S.P. Debbarma, R.K. Dutta, B. Mohanty, Pressure-settlement behavior of square and rectangular skirted footings resting on sand. Geomechanics and Engineering.**12**(4), 689-705 (2017)

[10] M. Örnek, M. Çalişici, Y. Türedi, N. Kaya, Investigation of skirt effect on eccentrically loaded model strip footing using laboratory tests. Soil Mechanics and Foundation Engineering, 58(3), 215-222. (2021).

[11] R. Alipour, J. Khazaei, M.S. Pakbaz, A. Ghalandarzadeh, Settlement control by deep and mass soil mixing in clayey soil. Proceedings of the Institution of Civil Engineers-Geotechnical Engineering, 170(1), 27-37. (2017).

[12] M.F. Bransby and M.F. Randolph. Combined loading of skirted foundation. Geotechnique, 48 (5), 637-655. (1998).

[13] B. W. Byrne and G. T. Houlsby. Experimental investigations of the response of suction caissons to transient vertical loading. J. Geotech. Geoenviron. Eng.128(11), 926–939. (2002).

[14] M. M. Dewoolkar, J. Hwang and H. Y. Ko. Physical and finite element modeling of lateral stability of offshore skirted gravity structures subjected to iceberg impact load. Ocean Eng.35(16), 1615–1626. (2008)

[15] S. Gourvenec, andK. Jensen. Effect of embedment and spacing of cojoined skirted foundation systems on undrained limit states under general loading. Int. J. Geomech.9(6), 267-279. (2009)

[16] C. Singh, J. Singh, S. Singh, V. Kumar, Performance of Inclined Skirt Footing: Numerical Analysis. In IOP Conference Series: Earth and Environmental Science. Vol. 889, No. 1, p. 012076. IOP Publishing. (2021)

[17] T. Gnananandarao, V.N. Khatri, R. K. Dutta, Performance of multi-edge skirted footings resting on sand. Indian Geotechnical Journal. (2017). DOI:10.1007/s40098-017-0270-6

[18] IS 1498 (1970) Classification and identification of soils for general engineering purposes. Bureau of Indian Standard

[19] T. Prasanth, P. Rajendra Kumar, A Study on Load Carrying Capacity of Skirted Foundation on Sand. International Journal of Science and Research, **6**(6), 2231-2235(2017)

[20] A.Z.E. Wakil, Bearing capacity of skirt circular footing on sand. Alexandria Engineering Journal, 52,359-364(2013)

[21] M. Y. Al-Aghbari, Y. E.-A. Mohamedzein, Improving the performance of circular foundations using structural skirts. Ground Improvement **10**(3), 125–132 (2006)

[22] D.S.K Mana "Numerical & experimental investigation of offshore shallow skirted foundations" Thesis report for Doctor of Philosophy of the university of western Australia, 2013

[23] A.S. Vesic, Analysis of ultimate loads of shallow foundations. Journal of the Soil Mechanics and Foundations Division.99, 45–73 (1973).